Electronic Supplementary Material (ESI) for RSC Advances.

Supplementary Information

to "Towards a better understanding of nickel/diamond interactions: the interface formation at low temperatures"

Boris B. Bokhonov, Arina V. Ukhina, Dina V. Dudina, Konstantin B. Gerasimov, Alexander G. Anisimov, Vyacheslav I. Mali

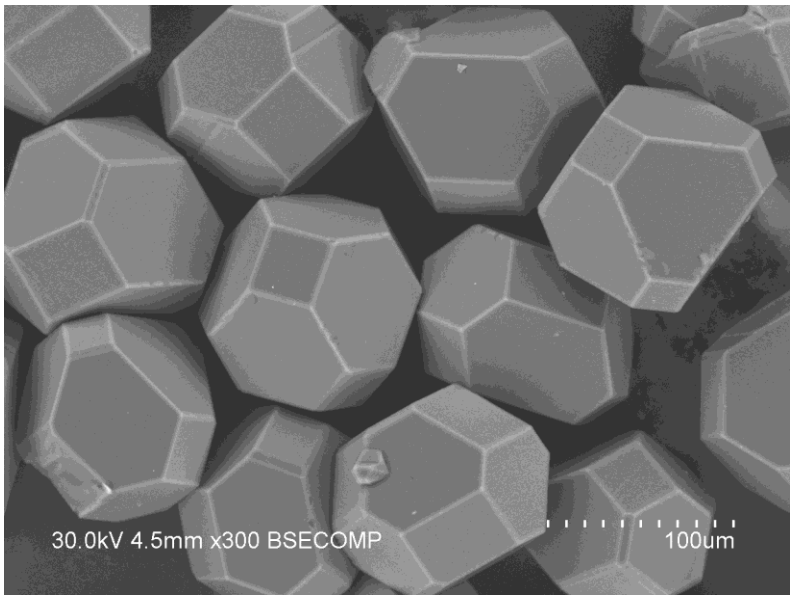

a

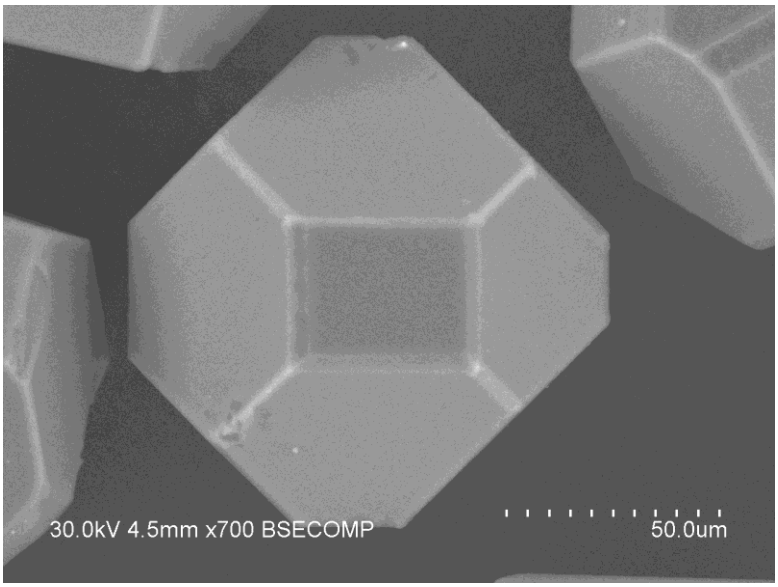

b

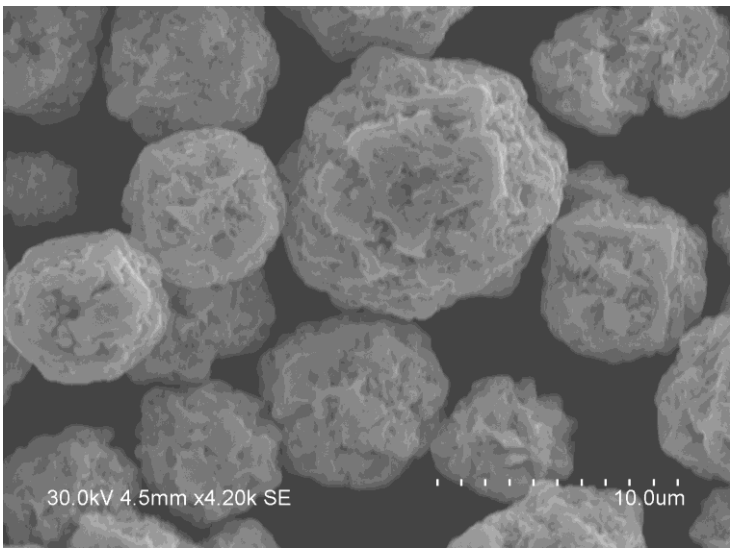

c

Figure 1S. Micrographs of the starting diamond (a-b) and nickel (c) powders.

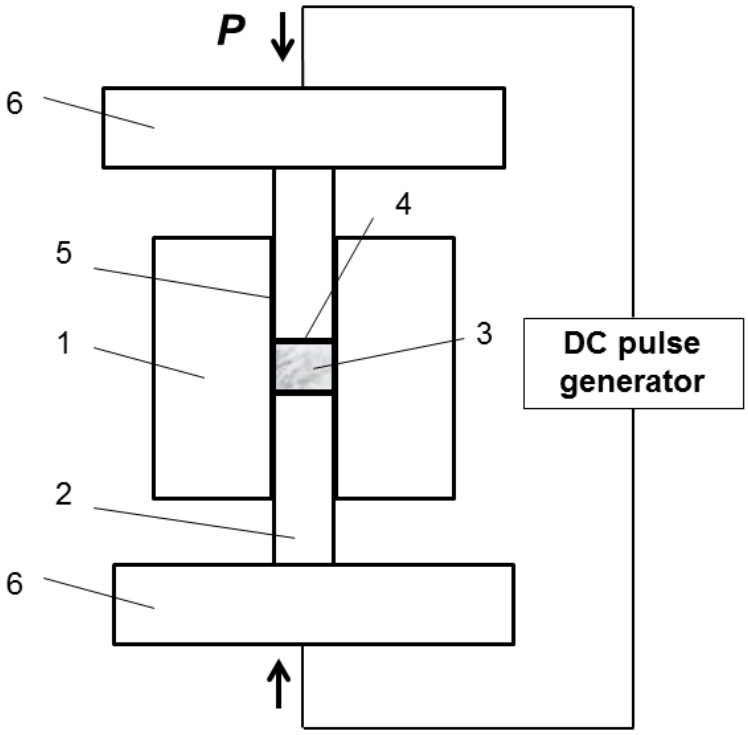

Figure 2S. A schematic of the die/punch assembly used in the Spark Plasma Sintering experiments (1 – graphite die, 2 – tungsten punch, 3 – sample, 4 – protective tantalum foil, 5 – protective graphite foil, 6 – graphite spacers). The assembly is placed in the vacuum chamber.

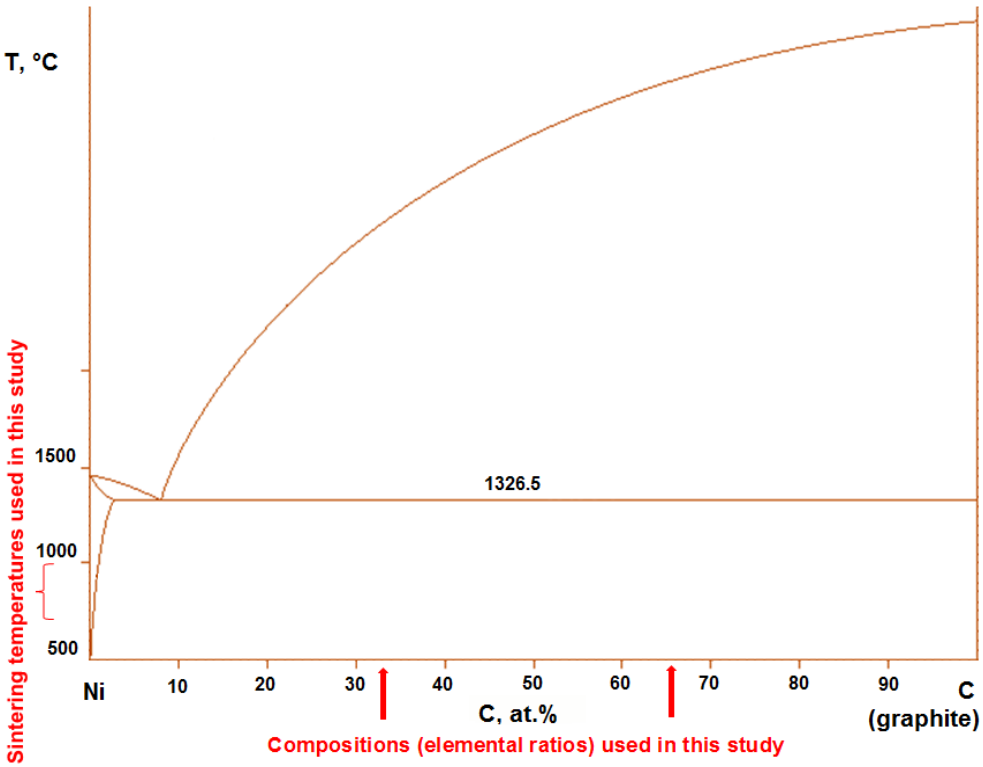

Figure 3S. Sintering temperatures and compositions of the nickel-diamond powder mixtures marked on the nickel-graphite phase diagram (the diagram is shown schematically according to M. Singleton and P. Nash, Alloy Phase Diagrams, 1989, 10, 121).

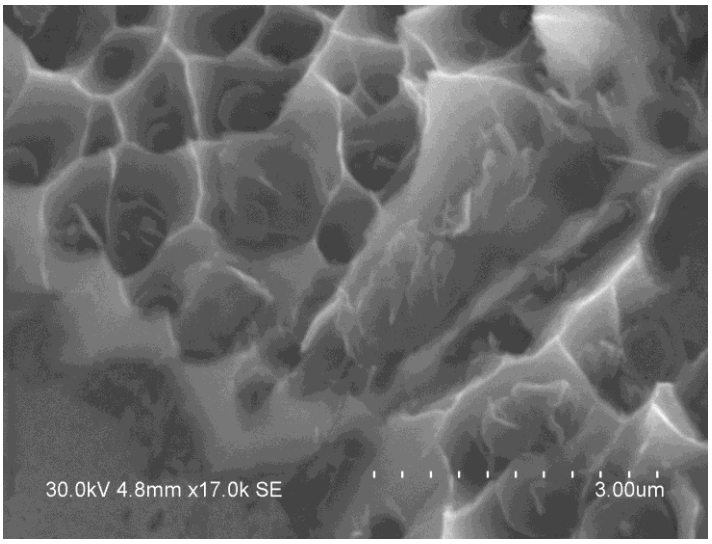

Figure 4S. Dimpled morphology of the fracture surface of the nickel-diamond inter-particle joints (patches on the diamond facets) observed in the nickel-diamond compact Spark Plasma Sintered at 900 °C.

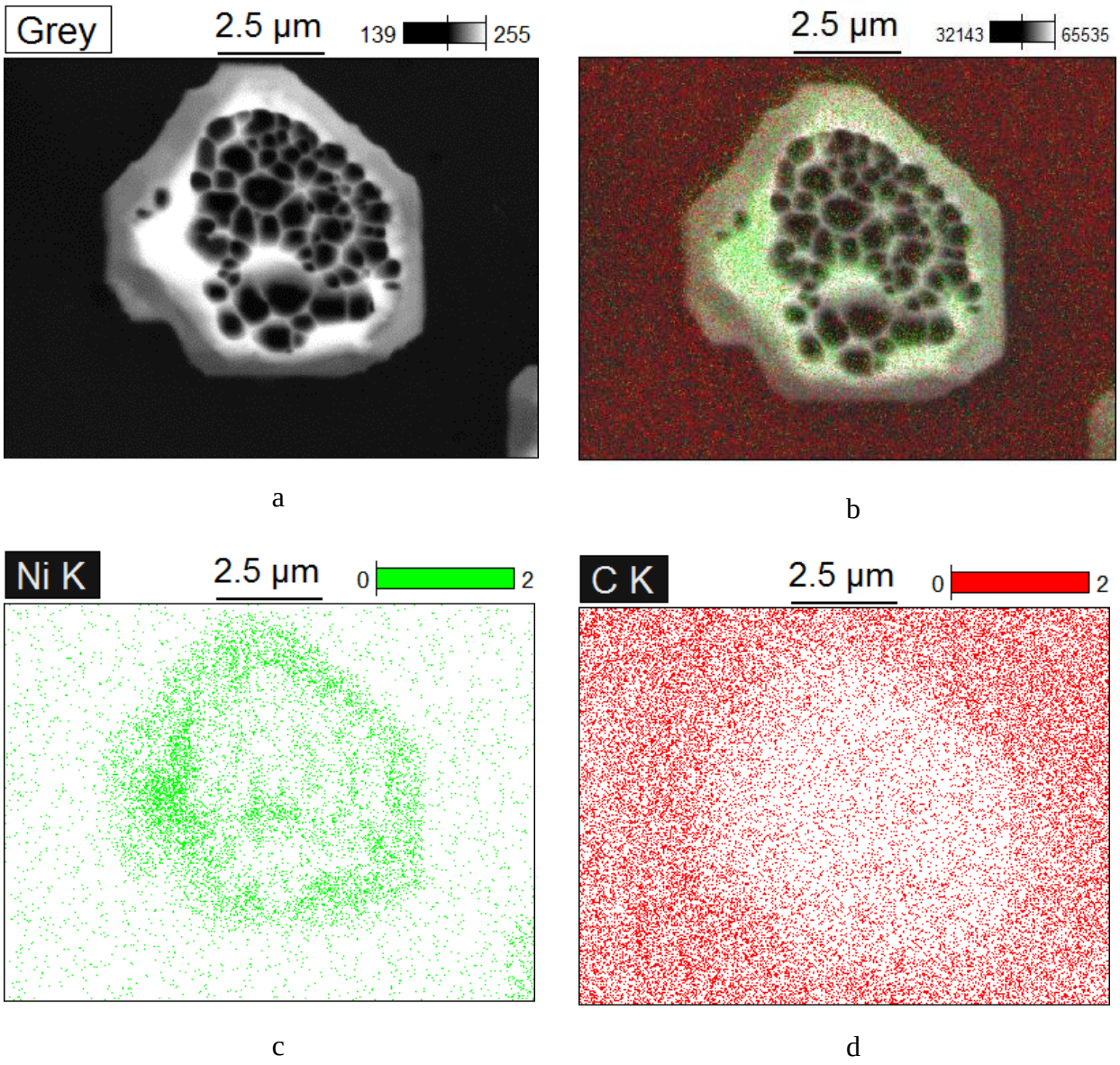

Figure 5S. Images (a-b) and elemental mapping (c-d) of a single patch on a (100) facet of a diamond particle in the nickel-diamond compact Spark Plasma Sintered at 900 °C.

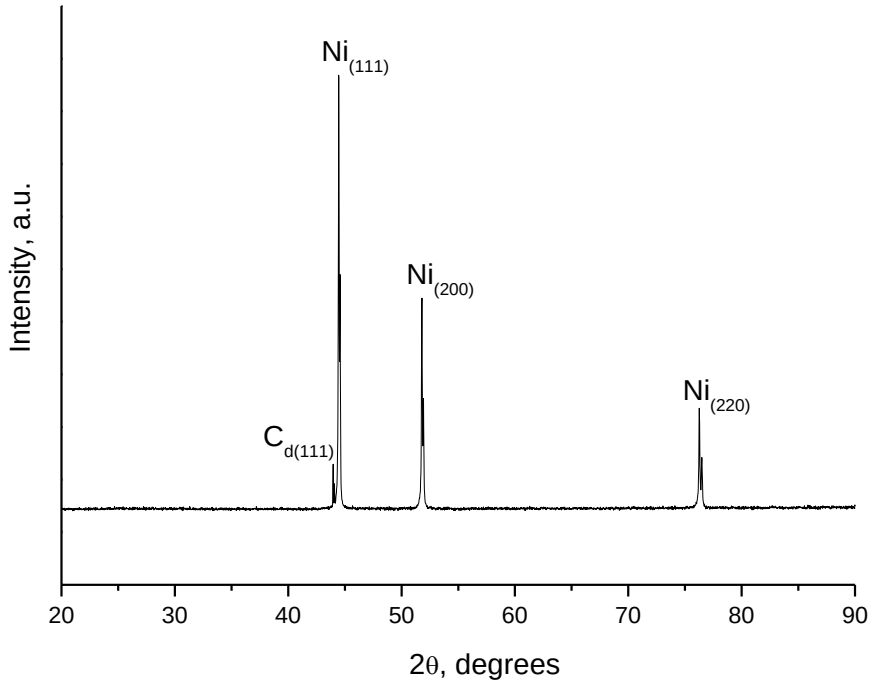

Figure 6S. XRD pattern of the nickel-diamond compact conventionally sintered at 900 °C.

Figure 7S. Fracture surface of the nickel-diamond compact hot pressed at 700 °C showing a (100) facet of a diamond particle with patches — a result of cohesive fracture of the nickel-diamond joints.

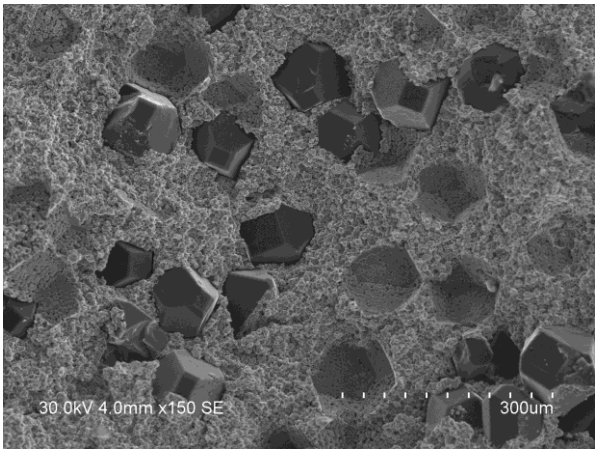

a

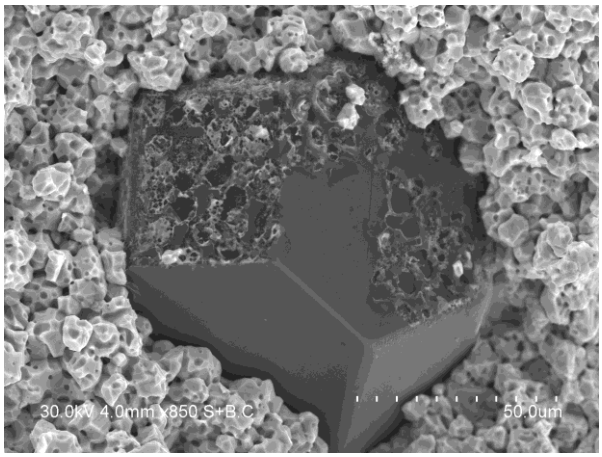

b

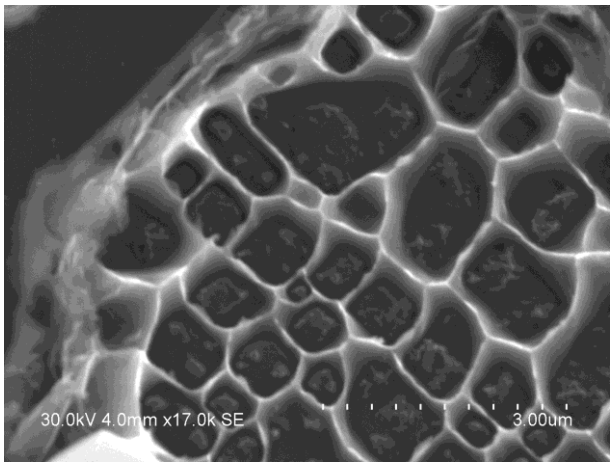

c

Figure 8S. A general view of the fracture surface of the nickel-diamond compact conventionally sintered at 900 °C (a), non-uniformly eroded diamond particle (b); fracture surface of the nickel-diamond joint (c).

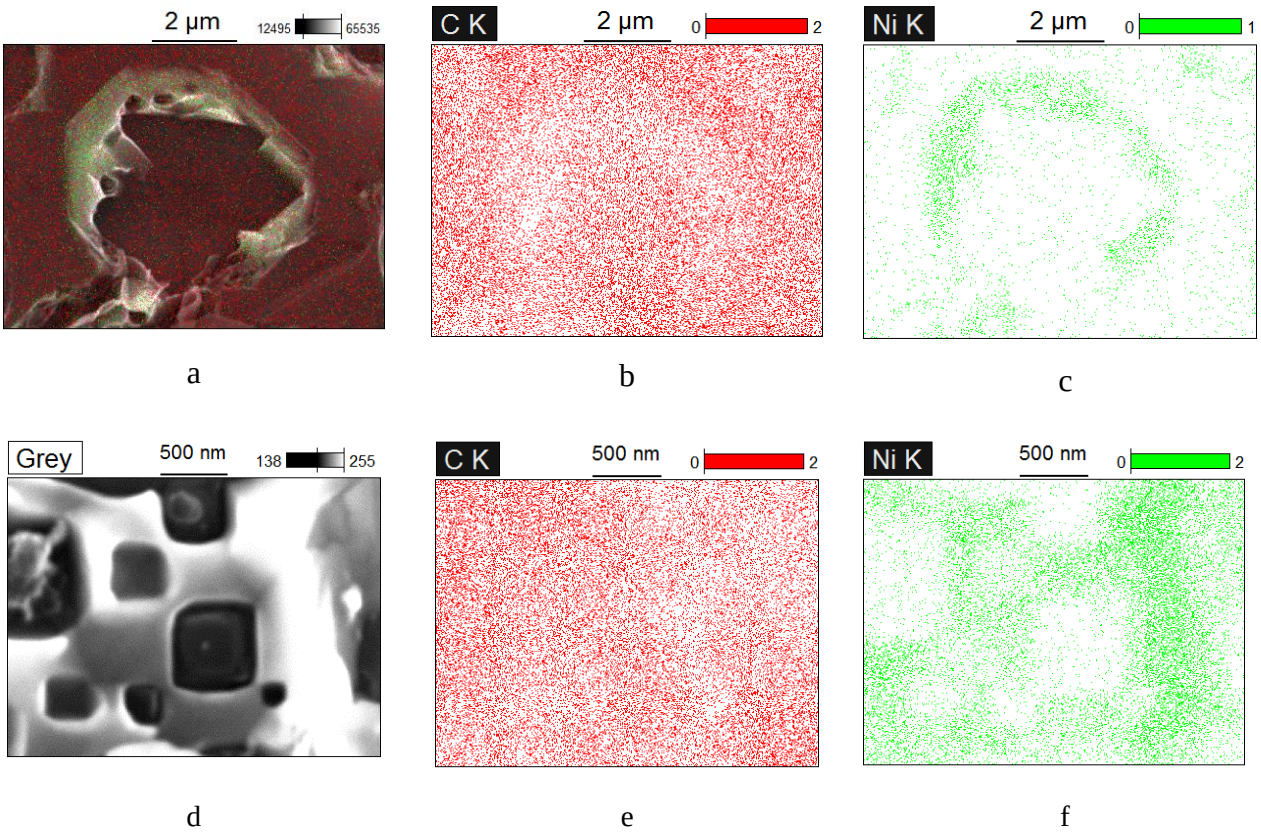

Figure 9S. Images (a, d) and elemental mapping (b-c, e-f) of a patch that formed as a result a nickel particle's adhering to a (100) facet of a diamond particle in the nickel-diamond compact conventionally sintered at 900 °C.

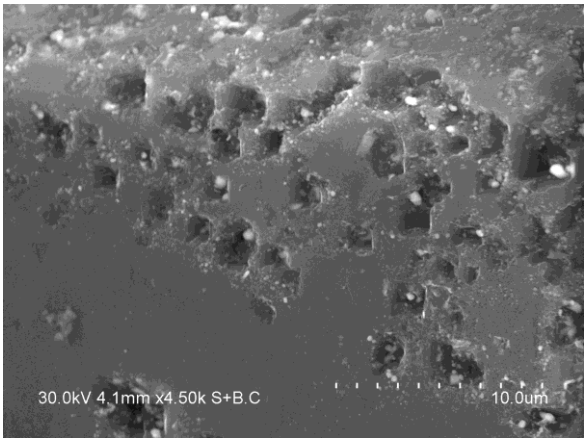

a

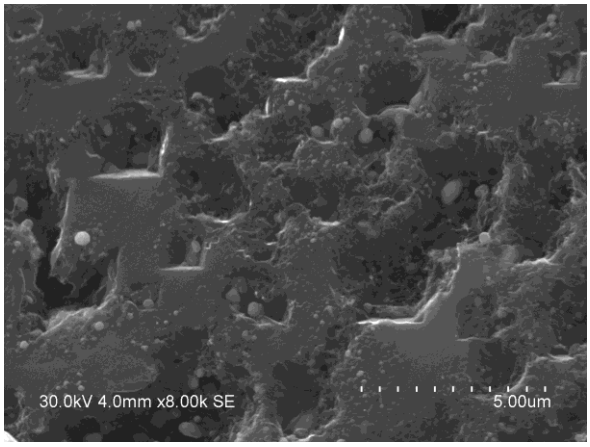

b

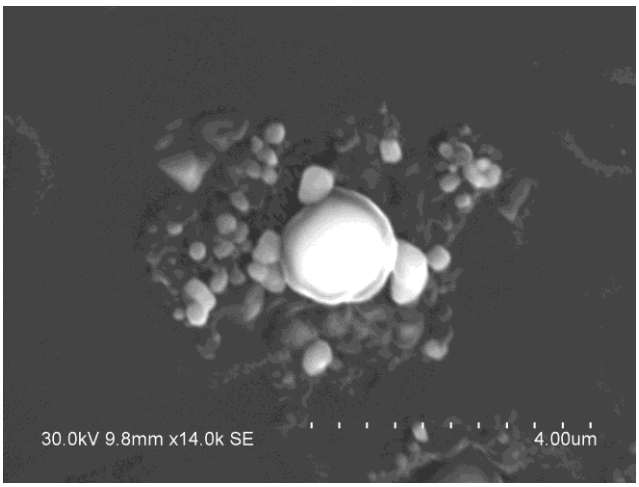

c

Figure 10S. Eroded surface of a diamond particle in the cold pressed iron-diamond compact annealed in vacuum at 900 °C for 1 h (a-b – different magnifications).

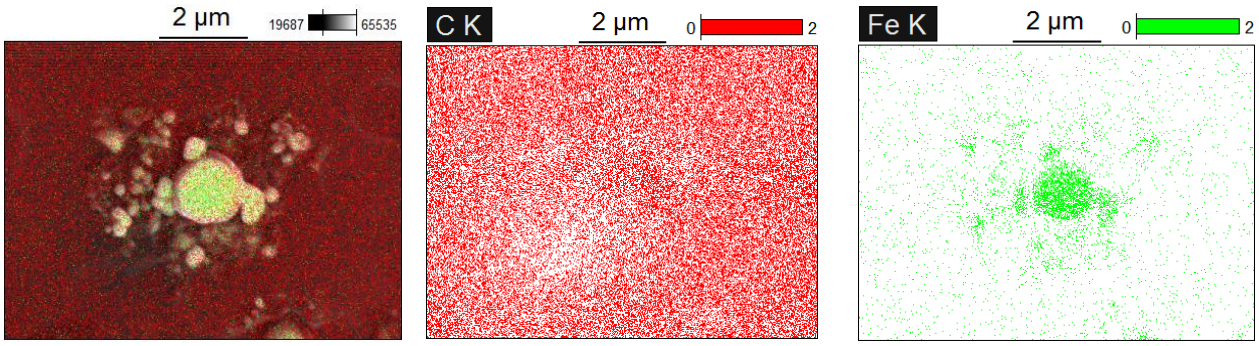

a b c

Figure 11S. Elemental mapping of a patch on a diamond particle in the iron-diamond compact conventionally sintered at 900 °C.

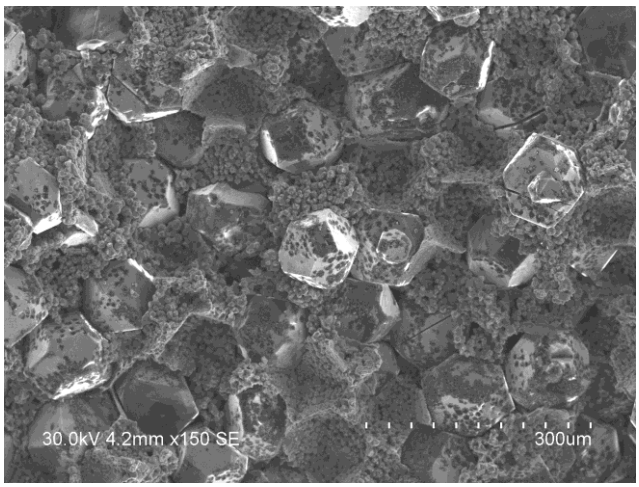

Figure 12S. A general view of the fracture surface of the nickel-diamond compact Spark Plasma Sintered at 900 °C after a DSC run in hydrogen up to 1300 °C.

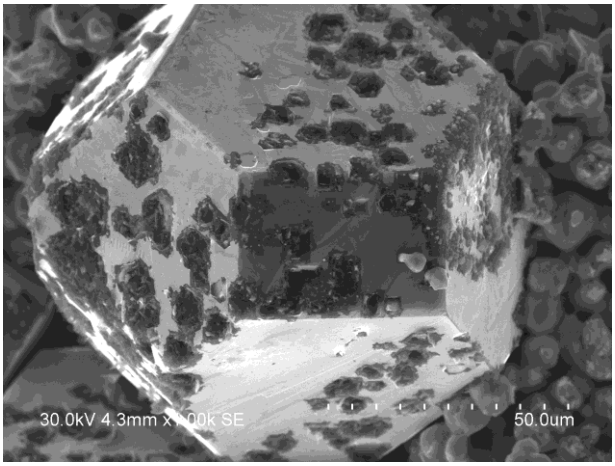

a

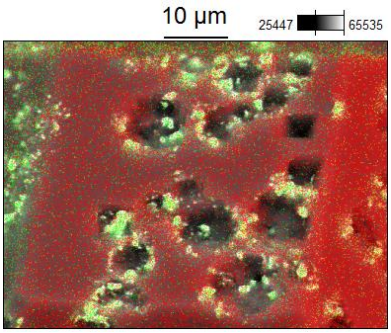

b

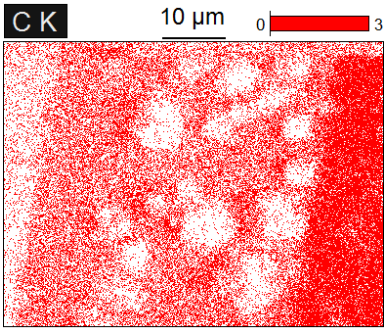

c

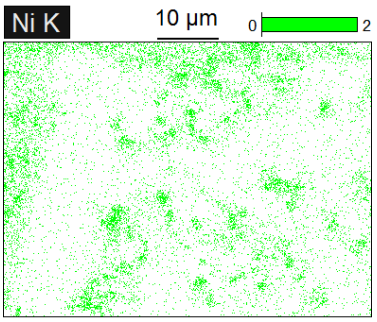

d

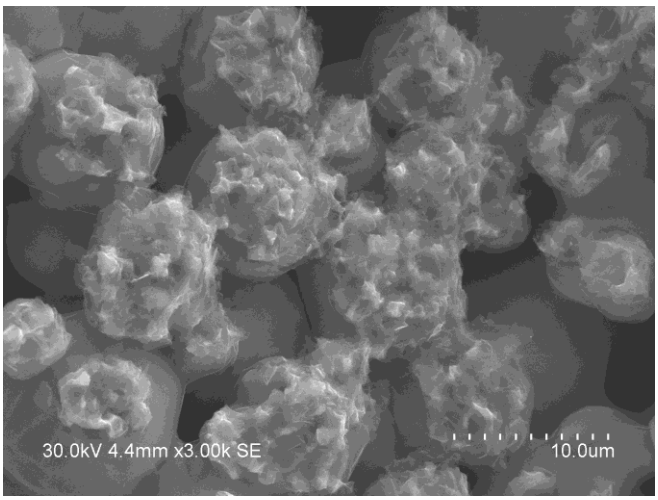

e

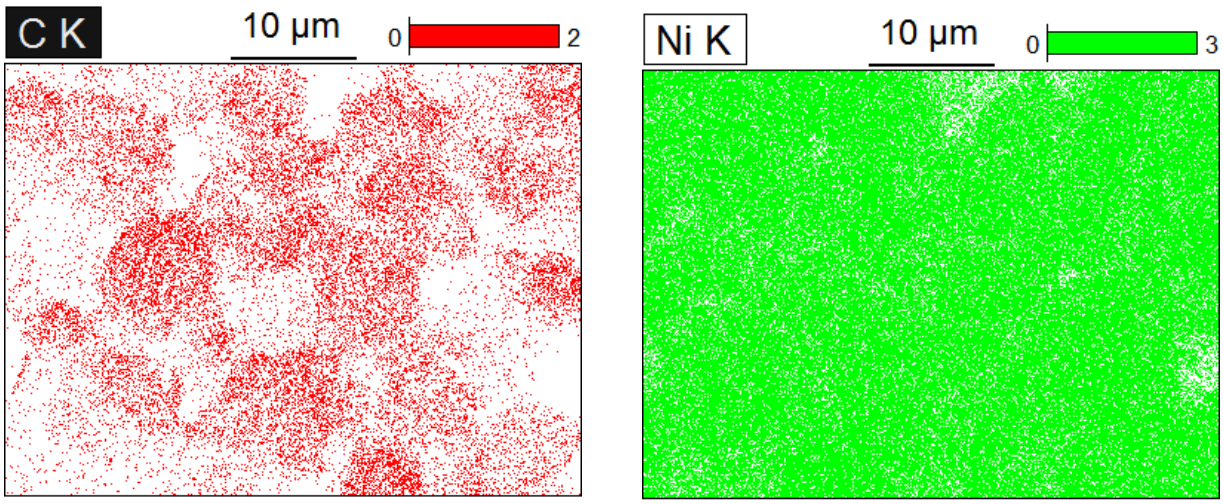

f g

Figure 13S. Fracture surface of the nickel-diamond compact Spark Plasma Sintered at 900 °C after a DSC run in hydrogen up to 1300 °C: etch pits (a-b) and elemental maps of carbon (c) and nickel (d) corresponding to (b); fracture surface of the nickel binder (e); elemental maps of carbon (f) and nickel (g) maps corresponding to (e).

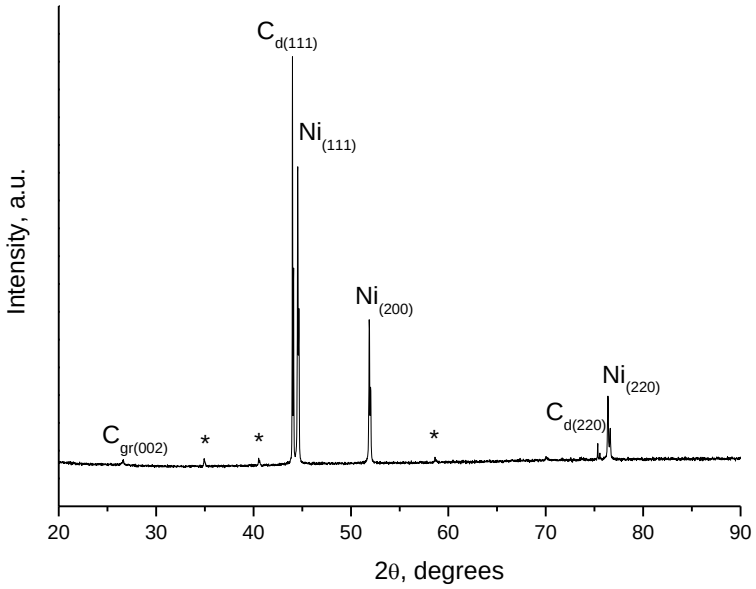

Figure 14S. XRD pattern of the nickel-diamond compact Spark Plasma Sintered at 900 °C after a DSC run in hydrogen up to 1300 °C, peaks marked with '*' are due to the presence of small amounts of tantalum carbide TaC formed as a results of interaction of the compact with the tantalum protecting foil.